Ultrafast two-step thermalization processes of photoexcited electrons at a gold surface: Application of a wavelength-selective transient reflecting grating method

Kenji Katayama, Yohei Inagaki, and Tsuguo Sawada*
Department of Advanced Materials Science, Graduate School of Frontier Sciences, The University of Tokyo, 7-3-1 Hongo, Bunkyo-ku, Tokyo 113-8656, Japan
(Received 1 November 1999)

We have observed two-step thermalization processes of photoexcited electrons in gold, by using a wavelength-selective transient reflecting grating method that provides information on carrier dynamics at each energy state selectively. We detected ultrafast processes around *L* and *X* points in the Brillouin zone. Within 1 ps, two relaxation components (40 ± 10 and 280 ± 40 fs) were observed only around *L*, and only the slower component was observed for every wavelength. We considered that the two relaxation processes occurred due to two kinds of electron-electron (*e-e*) scattering predicted from the Fermi-liquid theory, because their decay times are in good agreement with the times obtained from the theory. We concluded that faster and slower *e-e* scatterings physically correspond to the relaxations of the initially photoexcited electrons at the *L* point, and of nonthermalized electrons at various Brillouin-zone points, respectively.

In recent years, much attention has been drawn to femtosecond photoexcited carrier dynamics at solid surfaces, since it was found that they do not obey the Fermi distribution in a femtosecond time region[1–11] and that they are involved in some interfacial chemical reactions.[12–14] Such nonequilibrium electrons (NE's) come to a thermal equilibrium through electron-electron scattering (*e-e* scattering) within electron gas. Thereafter electrons whose temperature is still higher than that of the lattice are cooled down to the lattice temperature. The NE dynamics, that is, the thermalization processes, are not well understood, while the latter processes, electron-phonon coupling, have already been clarified in detail. The thermalization processes have been investigated with transient reflectivity (TR) and two-photon photoemission (2PPE) methods. It was reported from the TR results that the thermalization time is about 500 fs under the conditions of low-power and low-energy excitation.[2–5] On the other hand, the thermalization time measured with the 2PPE method ranges from dozens of femtoseconds to a few hundred.[6,7] Though both methods measure the same thermalization processes, the obtained thermalization times do not quantitatively agree. In this paper, we investigate the NE thermalization processes more fully using a transient reflecting grating (TRG) method. The TRG method, like the TR method, is an ultrafast photothermal measurement method, but it features a higher sensitivity than the TR method due to a lack of background detection.[15–21] This time, we improved the TRG method so as to allow selective monitoring of excited electrons at each energy state, like the 2PPE method, by adopting a white-light continuum as a probe pulse. Although this improved TRG method is an ultrafast spectroscopic method utilizing four-wave mixing, and has already been applied to solutions,[22,23] we have applied it to solid surfaces for the first time, to our knowledge.

In the TRG technique, two crossed-pump pulses are incident at a solid surface and, as a result, the focused spot is irradiated with a pulse of an interference pattern. The complex refractive index at the spot changes due to a physical property change. After the pump pulses irradiation, a probe pulse is also incident there, and the complex refractive index change is detected through the diffracted light of the probe light.[24] A complex permittivity is often used to express various physical properties of solids, and the measured complex refractive index is equal to the square of the complex permittivity. In the time region from femtoseconds to picoseconds, the complex permittivity changes in accordance with the energy distribution of photoexcited carriers, and the theoretical expressions are discussed as follows.

The complex permittivity has different expressions according to whether an interband transition occurs or not. In this study, we used a white-light continuum that includes wavelengths corresponding not only to an intraband transition, but also to an interband transition. If the energy for a wavelength is smaller than that of the interband transition, the complex permittivity is expressed from the classical Drude theory as[25]

$$\tilde{\varepsilon}(\omega)=1-\frac{\omega_p^2}{\omega(\omega+i/\tau)}, \tag{1}$$

where ω is the angular frequency of the probe light, ω_p is the plasma frequency of a sample, and τ is the relaxation time of free electrons. When pump pulses excite photoexcited electrons, the τ value is varied due to the change of the energy distribution of the electrons. Thus we can detect a complex permittivity change through the τ value.

For a wavelength corresponding to an interband transition, the Drude component of the complex permittivity becomes smaller in proportion to the square of the wavelength,[26] and instead a component of the complex permittivity arises, originating in an interband transition. This component mainly determines the complex permittivity value. In this case, the permittivity change depends on the carrier density at the upper and lower states of the interband transition. With regard to metals, photoexcited holes at the lower state have a much shorter lifetime than electrons, and

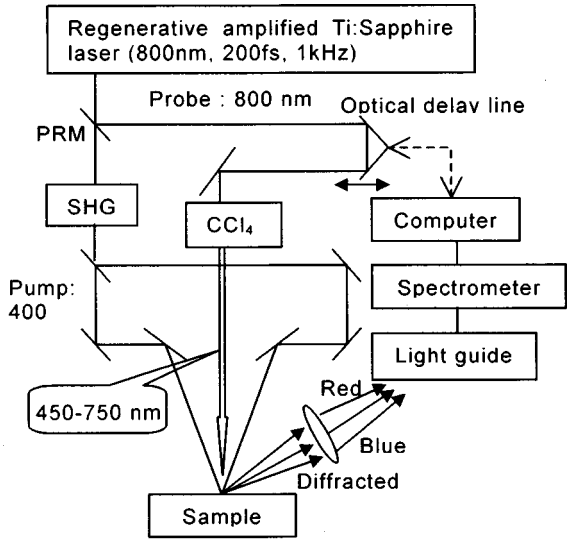

FIG. 1. Experimental arrangement for the transient reflecting grating method using a femtosecond white-light continuum probe pulse. The probe pulse was focused to the 10-mm-thick cell filled with carbon tetrachloride to generate a femtosecond white-light continuum (450–750 nm). The spread reflected diffracted light with a rainbow of colors was directed to the light guide after being focused by the lens. PRM is the partially reflective mirror, and SHG the nonlinear crystal.

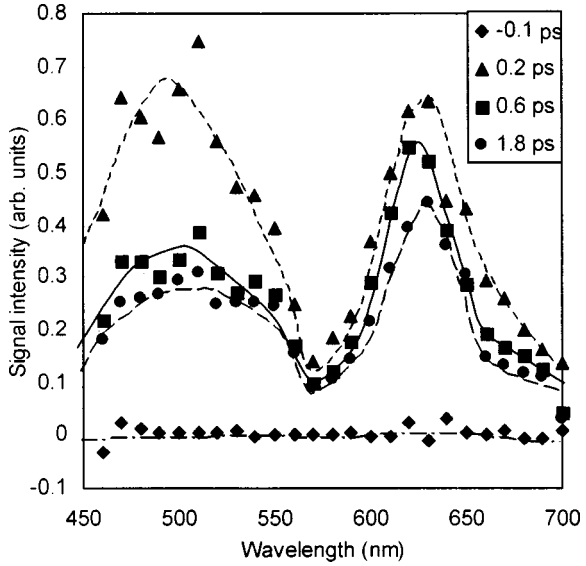

FIG. 2. Transient reflecting grating spectra at various probe delays. The measured sample was a vapor-deposited gold film (thickness 100 nm). For clarity of the spectrum shape, a smooth line is also shown for each delay time.

we neglect them here.[27] If we assume the carrier density fluctuation as $\Delta\rho$, the imaginary part of the complex permittivity changes as[2,28,29]

$$\Delta\varepsilon_2(\omega)=\frac{1}{(\hbar\omega)^2}\int D(E,\omega)\Delta\rho(E)dE, \qquad (2)$$

where $D(E,\omega)$ is the joint density of state. The real part of the complex permittivity also changes according to the Kramers-Kronig relation. Using our method, we can selectively observe the relaxation processes of free electrons or electrons at a focused energy state, if we select a probe wavelength corresponding to an intraband transition or an interband transition.

The TRG equipment is illustrated in Fig. 1. A regeneratively amplified titanium sapphire laser laser (CPA-1000: Clark-MXR Inc.) was used as a light source. The pulse train wavelength was 800 nm, with a repetition rate of 1 kHz and a pulse width of 230 fs, in full width at half maximum. The pulse was separated into pump and probe pulses using a partial reflective mirror. The pump pulses were frequency doubled to a wavelength of 400 nm (3.1 eV), and then further divided into two pulses by a half mirror. The two pump pulses were crossed and irradiated onto the same spot of the sample surface, to coincide in time to form an interference pattern. The pump intensity was less than 1 mJ/cm^2 per pulse at the sample. The probe pulse was focused to a 10-mm-thick cell filled with carbon tetrachloride to generate a femtosecond white-light continuum after passing through a computer-controlled optical delay line. Wavelengths used ranged from 450 nm (2.75 eV) to 750 nm (1.91 eV). The probe pulse was irradiated at the center of the spot. The reflected diffracted light with a rainbow of colors spread like a fan due to the diffraction conditions. It was directed to the entrance of the optical fiber end after being collected and focused by the lens. The diffraction spectrum was detected using the PMA-11 (HAMAMATSU) with a built-in spectroscope and CCD camera. The wavelength resolution of this equipment was 2 nm. TRG signals were obtained without using a box-car integrator or a lock-in amplifier; instead the signal was averaged at each point of the optical delay line. The measuring time for one typical TRG spectrum (200 points: 10 ps) was about 15 min. The polarizations of the pump and probe light were cross-polarized to prevent any coherent effects. The sample was a vapor-deposited gold film 100 nm thick, prepared with a vacuum coater, VPC-260 (ULVAC). The pressure and deposition speed were 1×10^{-3} Pa and 0.01 nm/s, respectively.

For the white-light continuum used this time, interband transitions occur at wavelengths shorter than 640 nm, but not longer than this. Thus comparison can be made between the signals for an interband transition and for an intraband transition. From detailed analyses of the gold band structure in the literature,[30–33] we can suppose that two interband transitions are involved in the probe wavelength region and they correspond to *d*-band to Fermi surface transitions at *X* and *L* in the Brillouin zone. Their absorptions begin from 1.94 eV (640 nm) and 2.45 eV (507 nm), respectively. On the other hand, the pump pulse (400 nm: 3.1 eV) generates photoexcited carriers mainly only due to the *L* transition.

The TRG spectrum at each delay time is shown in Fig. 2. There are two peaks at 510 nm (2.5 eV) and 620 nm (2.0 eV), and the signal intensity rises to a maximum at 0.2 ps for every wavelength. The peaks at 510 and 620 nm show a different temporal tendency. It is clear that the former has a faster relaxation component. We may consider that the signal at each peak corresponds to an electron density change in the vicinity of the Fermi surface at *X* and *L*, because the position of each peak is in good agreement with each transition. The maximums of the two peaks are more than five times larger

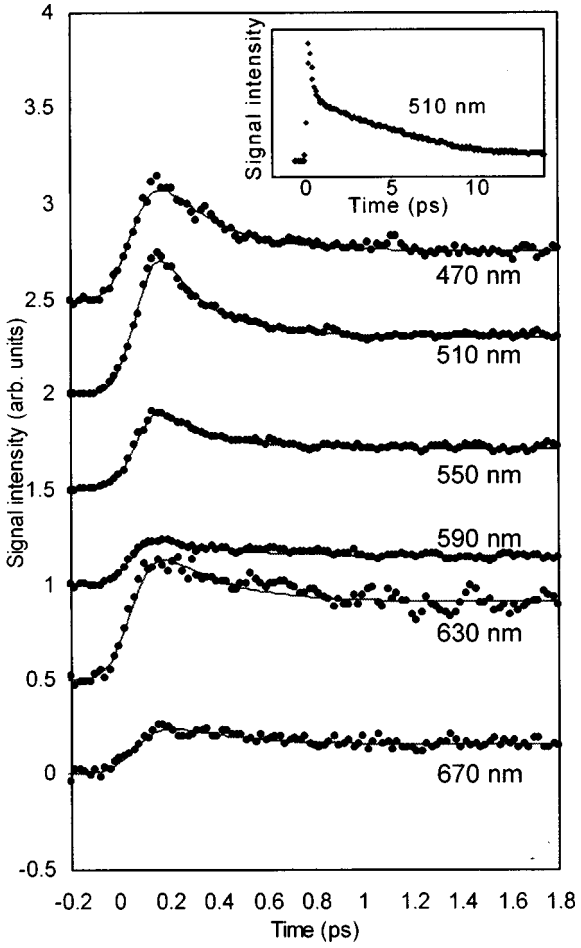

FIG. 3. Transient reflecting grating responses and fitted curves for various probe wavelengths up to 1.8 ps. Each wave form is vertically displaced for clarity. The measured sample was a vapor-deposited gold film (thickness 100 nm). The inset shows a typical transient reflecting grating response up to 15 ps (probe wavelength 510 nm).

in intensity than at 700 nm, the wavelength for the intraband transition. This means the refractive index change in Eq. (2) is larger than that in Eq. (1).

To clarify the signal decay, we show some TRG responses at typical wavelengths in Fig. 3. Furthermore, a typical TRG response for 510 nm is given until 15 ps in the inset. This response shows a 10 ps linear decay, and the decay is observed for every wavelength. Compared with results in the literature,[2–4,34] we can consider that the linear decay corresponds to the temperature fall of photoexcited electrons due to electron-phonon scattering. It was proved using the two-temperature model that this component decays linearly, when the temperature of photoexcited electrons is much higher than that of phonons.[35] Looking at TRG responses within 1 ps we observe two relaxation components around 510 nm, that is, the transition at L, while only the slower component is observed for every wavelength. We made a curve fitting to estimate the time constants. The square root of a TRG signal was fitted because the signal is proportional to the square of the refractive index change. The convoluted function of a double exponential decay plus a constant with the incident pulse was used as a fitting function. The wave forms for every wavelength can be fitted with 40 ± 10 and 280 ± 40 fs. The ratio of 40-fs component in the wave forms increases as the wavelength draws nearer to 510 nm, and decreases moving away from it. For wavelengths longer than 550 nm, only the 280-fs component is included in the wave forms.

Since these relaxations occurred before electron-phonon coupling, we can suppose that the processes correspond to the NE thermalization due to *e-e* scattering. As mentioned above, NE thermalization dynamics has been measured with the 2PPE and TR methods, but the reported thermalization times measured with each method do not agree [2PPE goes from dozens to a few hundred femtoseconds,[6,7] and TR typically is 500 fs (Refs. 2–5)]. Also, a two-step relaxation like this result has never been observed. Then we reconsidered Fermi-liquid theory which has been used for an explanation of the thermalization processes. The thermalization time due to *e-e* scattering is predicted from theory as[5]

$$\frac{1}{\tau_e}=K\frac{(\pi k_B T_e)^2+\varepsilon^2}{1+\exp(-\varepsilon/k_B T_e)}, \tag{3}$$

where T_e is the electron temperature at the conduction band, ε is the energy of a focused electron measured from the Fermi energy, and K is the *e-e* scattering constant. Considering that the pump beams (3.11 eV) excite electrons around the transition at L (2.45 eV), ε equals 0.66 eV just after photoexcitation, which is much larger than $k_B T_{e'}$, and then Eq. (3) is approximated as $1/\tau_e \approx K\varepsilon^2$. This equation physically means that the phase space in the energy range of ε is available for *e-e* scattering processes. As time passes, the NE's around the L point distribute their energy to all other electrons due to *e-e* scattering. When their energy is reduced to $k_B T_{e'}$ Eq. (3) is approximated as $1/\tau_e \approx K(\pi k_B T_e)^2$, which physically means available phase space in the energy range of $k_B T_e$. From these considerations, we now see that two processes are involved in the thermalization processes due to *e-e* scattering.

Using the above approximated equation, the relaxation time due to the faster *e-e* scattering is estimated to be 42 fs with $K=0.055\,(\mathrm{eV/fs^{-1}})$,[4] and that due to the slower *e-e* scattering is calculated as 310 fs with the K and $\tau_e = 960\,\mathrm{K}$; τ_e is obtained from the absorbed energy per volume: $2.7\times10^7\,(\mathrm{J\,m^{-3}pulse^{-1}})$, and the electronic specific heat $66T_e\,(\mathrm{J\,m^{-3}\,K^{-1}})$. We can conclude that the two observed relaxations correspond to the thermalization processes due to the above-mentioned two kinds of *e-e* scattering, because of the good agreement between the theoretical and experimental time constants. Further, we suggest that the 2PPE and TR methods have measured the thermalization processes for the faster and slower *e-e* scattering, respectively.

We note that the relaxation due to the faster *e-e* scattering is observed only around the transition at L, while the slower *e-e* scattering is observed for every wavelength. These results indicate that the faster *e-e* scattering occurs only around L, while the NE's dissipate their energy to other electrons to make other NE's in various regions of the Brillouin zone. Thus the slower *e-e* scattering is observed for every wavelength. We summarize the relaxation phenomena as follows: First, the pump beam (3.11 eV) excites electrons at the L point in the Brillouin zone to about 0.66 eV above the Fermi

level. Second, the relaxation of NE's occurs due to the faster *e-e* scattering in the vicinity of *L*, and the dissipated energy is distributed to other electrons in various regions of the Brillouin zone (40 fs). Third, the newly generated NE's thermalize and show a Fermi distribution (280 fs). Finally, the raised temperature of the electrons falls due to electron-phonon scattering (10 ps). In this study, we made two important points. (1) We detected two-step NE thermalization processes due to two kinds of *e-e* scattering. (2) We showed that the thermalization processes were different at each Brillouin-zone point, by selectively monitoring each transition band.

*Electronic address: sawadat@laser.t.u-tokyo.ac.jp FAX: +81-3-5841-6037.

[1] W. S. Fann, R. Storz, H. W. K. Tom, and J. Bokor, Phys. Rev. B **46**, 13 592 (1992).
[2] C. K. Sun, F. Vallee, L. H. Acioli, E. P. Ippen, and J. G. Fujimoto, Phys. Rev. B **50**, 15 337 (1994).
[3] C. K. Sun, F. Vallee, L. Acioli, E. P. Ippen, and J. G. Fujimoto, Phys. Rev. B **48**, 12 365 (1993).
[4] R. H. M. Groeneveld, R. Sprik, and A. Lagendijk, Phys. Rev. B **51**, 11 433 (1995).
[5] R. H. M. Groeneveld, R. Sprik, and A. Lagendijk, Phys. Rev. B **51**, 5079 (1992).
[6] J. Cao, Y. Gao, R. J. D. Miller, H. E. Elsayed-Ali, and D. A. Mantell, Phys. Rev. B **58**, 10 948 (1998).
[7] M. Aeschlimann, M. Bauer, and S. Pawlik, Chem. Phys. **205**, 127 (1996).
[8] W. S. Fann, R. Storz, H. W. K. Tom, and J. Bokor, Phys. Rev. Lett. **68**, 2834 (1992).
[9] S. Xu, J. Cao, C. C. Miller, D. A. Mantell, R. J. D. Miller, and Y. Gao, Phys. Rev. Lett. **76**, 483 (1996).
[10] R. W. Schoenlein, J. G. Fujimoto, G. L. Eesley, and T. W. Capehart, Phys. Rev. B **43**, 4688 (1991).
[11] J. Cao, Y. Gao, R. J. D. Miller, H. E. Elsayed-Ali, and D. A. Mantell, Phys. Rev. B **56**, 1099 (1997).
[12] A. Harata, T. Edo, and T. Sawada, Chem. Phys. Lett. **249**, 112 (1996).
[13] A. Hibara, A. Harata, and T. Sawada, Chem. Phys. Lett. **272**, 1 (1997).
[14] T. Morishita, A. Hibara, I. Tsuyumoto, and T. Sawada, J. Phys. Chem. B **103**, 5984 (1999).
[15] A. Harata, H. Nishimura, and T. Sawada, Appl. Phys. Lett. **57**, 132 (1990).
[16] I. M. Fishman, C. D. Marshall, A. Tokmakoff, and M. D. Fayer, J. Opt. Soc. Am. B **10**, 1006 (1993).
[17] A. R. Duggal, J. A. Rogers, and K. A. Nelson, J. Appl. Phys. **72**, 2823 (1992).
[18] A. Hibara, T. Morishita, I. Tsuyumoto, A. Harata, T. Kitamori, and T. Sawada, Jpn. J. Appl. Phys., Part 1 **38**, 2983 (1999).
[19] Q. Shen, A. Harata, and T. Sawada, J. Appl. Phys. **77**, 1488 (1995).
[20] K. Katayama, Q. Shen, A. Harata, and T. Sawada, Appl. Phys. Lett. **69**, 2468 (1996).
[21] K. Katayama, Q. Shen, A. Harata, and T. Sawada, Phys. Rev. B **58**, 8428 (1998).
[22] W. P. deBoeij, M. S. Pshenichnikov, and D. A. Wiersma, Annu. Rev. Phys. Chem. **49**, 99 (1998).
[23] W. P. deBoeij, M. S. Pshenichnikov, and D. A. Wiersma, Chem. Phys. **233**, 287 (1998).
[24] A. Harata and T. Sawada, Trends Analytical Chem. **14**, 504 (1995).
[25] J. Hohlfeld, D. Grosenick, U. Conrad, and E. Matthias, Appl. Phys. A: Mater. Sci. Process. **60**, 137 (1995).
[26] M. L. Theye, Phys. Rev. B **2**, 3060 (1970).
[27] M. Perner, P. Bost, U. Lemmer, G. von Plessen, J. Feldmann, U. Becker, M. Mennig, M. Schmitt, and H. Schmidt, Phys. Rev. Lett. **78**, 2192 (1997).
[28] R. Rosei, Phys. Rev. B **10**, 474 (1974).
[29] R. Rosei, C. H. Culp, and J. H. Weaver, Phys. Rev. B **10**, 484 (1974).
[30] M. Welkowsky and R. Braunstein, Solid State Commun. **9**, 2139 (1971).
[31] R. Rosei, F. Antonangeli, and U. M. Grassano, Surf. Sci. **37**, 689 (1973).
[32] M. Guerrisi, R. Rosei, and P. Winsemius, Phys. Rev. B **12**, 557 (1975).
[33] P. Winsemius, M. Guerrisi, and R. Rosei, Phys. Rev. B **12**, 4570 (1975).
[34] R. W. Schoenlein, W. Z. Lin, J. G. Fujimoto, and G. L. Eesley, Phys. Rev. Lett. **58**, 1680 (1987).
[35] J. Hohlfeld, J. G. Muller, S. S. Wellershoff, and E. Matthias, Appl. Phys. B: Lasers Opt. **64**, 387 (1997).